9-1-2009

Electric Field Enhancement of Electron Emission Rates from Z(1/2) Centers in 4H-SiC

A. O. Evwaraye

S. R. Smith

William C. Mitchel

Gary C. Farlow
Wright State University - Main Campus, gary.farlow@wright.edu

Electric field enhancement of electron emission rates from $Z_{1/2}$ centers in 4*H*-SiC

A. O. Evwaraye,[1,a)] S. R. Smith,[2] W. C. Mitchel,[3] and G. C. Farlow[4]
[1]*Department of Physics, University of Dayton, 300 College Park, Dayton, Ohio 45469-2314, USA*
[2]*University of Dayton Research Institute, 300 College Park, Dayton, Ohio 45469-0178, USA*
[3]*Air Force Research Laboratory, 3005P Street, Wright-Patterson Air Force Base, Ohio 45433-7707, USA*
[4]*Department of Physics, Wright State University, 3640 Col. Glenn Hwy, Dayton, Ohio 45435, USA*

(Received 21 April 2009; accepted 12 August 2009; published online 18 September 2009)

$Z_{1/2}$ defect centers were produced by irradiating 4*H*-SiC bulk samples with 1 MeV electrons at room temperature. The emission rate dependence on the electric field in the depletion region was measured using deep level transient spectroscopy and double-correlation deep level transient spectroscopy. It is found that the $Z_{1/2}$ defect level shows a strong electric field dependence with activation energy decreasing from $E_c-0.72$ eV at zero field to $E_c-0.47$ eV at 6.91×10^5 V/cm. The phonon assisted tunneling model of Karpus and Perel [Sov. Phys. JETP **64**, 1376 (1986)] completely describes the experimental data. This model describes the dependence of the emission rate on electric field F as $e_n(F)=e_{no}\exp(F^2/F_c^2)$, where F_c is the characteristic field that depends on the phonon assisted tunneling time τ_2. The values of F_c and τ_2 were determined and the analysis of the data leads to the suggestion that $Z_{1/2}$ may be a substitutional point defect. © *2009 American Institute of Physics*. [doi:10.1063/1.3224872]

I. INTRODUCTION

Irradiation induced defects and impurity defects in 4*H*-SiC have been extensively studied using deep level transient spectroscopy (DLTS).[1–12] The prominent feature of a standard DLTS thermal scan of irradiation induced defects in 4*H*-SiC samples is the $Z_{1/2}$ center. The $Z_{1/2}$ center is also observed in as grown epitaxial layers.[9] The center consists of a pair of defects (Z_1 and Z_2) with closely spaced electrical levels; both defects have negative U properties having inverted donor and acceptor levels and possess unusual thermal stability surviving up to 2000 °C according to the recent isochronal annealing experiments of Alfieri *et al.*[13] The donor level[7,14] of $Z_1(Z_2)$ occurs at $E_c-0.43$ eV ($E_c-0.46$ eV) and the acceptor level at $E_c-0.67$ eV ($E_c-0.71$ eV). The donor levels are not normally observed in the standard DLTS scan; the dominant feature that is observed in the DLTS experiments is due to the acceptor levels of Z_1 and Z_2. It is well known that the center exists in three different charge states.[10] It is positively charged ($Z_{1/2}^+$) when it is not occupied by an electron; it is negatively charged when it is occupied by two electrons ($Z_{1/2}^-$) and it is neutral when occupied by one electron. This is summarized as $Z_{1/2}^{-/0/+}$. The DLTS peak associated with $Z_{1/2}$ center is due to the overlapping two-electron emissions from both Z_1 and Z_2 defects, i.e., $Z_1^{-/0}\rightarrow Z_1^{0/+}+e$; $Z_2^{-/0}\rightarrow Z_2^{0/+}+e$. The center $Z_{1/2}$ is neutral and it is a nonionized donor after the electron emissions. Therefore, the emission processes from $Z_{1/2}^{-/0}$ defect should not be sensitive to the Poole–Frenkel mechanism.[15] The Poole–Frenkel effect describes the increase in the thermal emission rate from a defect in an external electric field by lowering the Coulomb barrier. This mechanism occurs only for charged defects. As far as we know, no Poole–Frenkel effect has been reported for $Z_{1/2}$ centers in 4*H*-SiC (Ref. 16) or electric field enhancement of emission rates from $Z_{1/2}$ centers in 4*H*-SiC. However, it must be noted that most studies (mainly characterization, annealing behavior, and attempts to identify its microscopic structure) of $Z_{1/2}$ centers have utilized epitaxial layers with net doping concentration of $6\times10^{13}-6\times10^{15}$ cm^{-3} as their samples. Castaldini *et al.*[16] as an example studied the $Z_{1/2}$ centers in a proton irradiated samples with net doping concentration of 4.5×10^{15} cm^{-3}. Their results show that the DLTS peak did not shift in temperature when the reverse bias was changed from −2 to −8 V. At these low doping concentrations, and with a typical reverse bias of 2–8 V, the electric field at the junction is too small ($<10^4$ V/cm) to produce enhancement of emission rates from a deep center. There are two other mechanisms, besides the Poole–Frenkel effect, that can account for an electric field enhancement of thermal emission rates from deep centers. These are phonon assisted tunneling and direct tunneling mechanisms. Both the phonon assisted tunneling and direct tunneling occur for defects in any charge state. However, direct tunneling occurs for electric fields in excess of 10^7 V/cm.

The purpose of this work is to produce $Z_{1/2}$ centers in a bulk 4*H*-SiC samples that have high net doping concentration of $(1-3)\times10^{17}$ cm^{-3} with 1 MeV electron irradiation. The high doping concentration assures, at a reverse bias of 1–13 V, high electric fields at the junction. The DLTS measurements and double-correlation deep level transient spectroscopy[17] (DDLTS) will be used to study in detail the effect of electric field on thermal emission rates from $Z_{1/2}$ centers in 4*H*-SiC.

II. EXPERIMENTAL PROCEDURE

The *n*-type bulk 4*H*-SiC wafers with a net doping concentration of 2.5×10^{17} cm^{-3} were obtained from Cree Inc.

a)Electronic mail: andrew.evwaraye@notes.udayton.edu.

The wafers were sliced into 0.25×0.25 cm^2 squares and Schottky diodes were fabricated onto the squares. These devices were then irradiated with 1 MeV electrons to fluences ranging from 1.0×10^{16} to 5.1×10^{17} e^-/cm^2. The current density during irradiation was kept at 0.91 μA/cm^2; this was to avoid heating the devices during irradiation. The temperature of the device did not rise more than 15 °C during irradiation. It is well known that electron irradiation of 4*H*-SiC samples produces several defects but $Z_{1/2}$ and $EH_{6/7}$ centers are the most thermally stable.[6,8,13] For these studies, the irradiated samples were annealed at 500 °C for 60 min. After the annealing, the DLTS peak associated with $Z_{1/2}$ defect is the only observed peak in a DLTS thermal scan from 200 to 380 K. All the other defects with activation energies smaller than that of the $Z_{1/2}$ center have annealed out.

The magnitude of the electric field in the space charge region varies linearly from a maximum of $F_m=qN_dx_d/\varepsilon_s$ to zero at the edge of the region where N_d is the net donor concentration and x_d is the depletion width. The λ-correction has been ignored.[18] The field at location x in the depletion region is $F_x=F_m[1-(x/x_d)]$. The dependence of the emission rate on the electric field was studied using the DDLTS. In this technique for a given reverse bias V_R, two filling pulses are utilized. The filling pulse V_{p1} produces a capacitance transient corresponding to defects spatially located between x_1 and x_d. The electric field at x_1 is $F_1=F_m[1-(x_1/x_d)]$.This pulse is followed by a second filling pulse V_{p2} ($V_{p2}>V_{p1}$), which now produces a capacitance transient corresponding to defects located between x_2 and x_d. These transients are subtracted from one another to produce a "difference" transient which gives the contribution of the defects filled in the x_2-x_1 region. If $V_{p2}-V_{p1}$ is small enough, the emission rates can be considered to be occurring in a constant electric field which is the average of F_1 and F_2. The emission rates and the activation energy can be extracted from the difference spectrum. $V_{p2}-V_{p1}$ was kept at 0.6 V throughout the experiment. By changing V_{p2} and V_{p1} but keeping ΔV_p at 0.6 V and V_R fixed, emission rates at a different electric field can be monitored. This method changes the electric field at which defects are probed but at different spatial locations. In order to probe defects in the same spatial location, the values of V_{p1} and V_{p2} are kept fixed and the reverse bias V_R is changed. Since the defect under study is uniformly distributed throughout the depletion region, both methods of changing the electric field yield identical results.

III. RESULTS AND DISCUSSION

Figure 1 shows the DLTS spectrum that was recorded with a rate window of 23.25 s^{-1} on a 4*H*-SiC sample that was annealed at 500 °C for 60 min after it was irradiated with 1 MeV electrons. The activation energy of $E_c-0.60$ eV and the capture cross section $\sigma=1.1\times10^{-14}$ cm^2 of the dominant peak were calculated from $\ln(e_n/T^2)$ versus $1/kT$ plot (see the inset). These values are in good agreement with reported values for the $Z_{1/2}^{/0}$ center. The dominant peak in Fig. 1 is therefore associated with electron emission from the $Z_{1/2}^{/0}$ center.

Figure 2 shows the three normalized DLTS spectra with

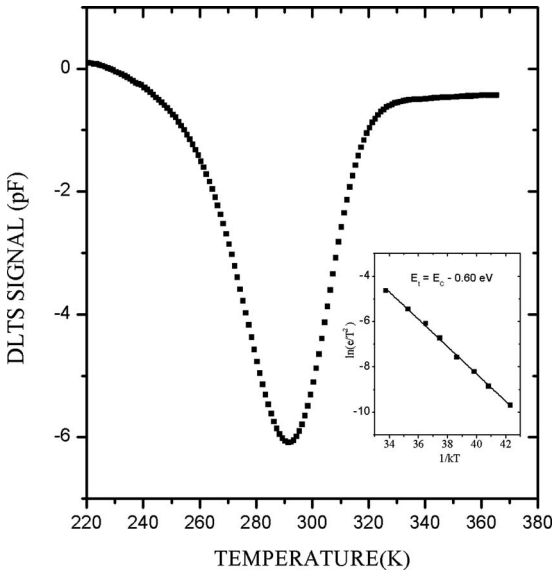

FIG. 1. DLTS spectrum obtained from 1 MeV electron irradiated *n*-type bulk 4*H*-SiC for an emission rate of 23.25 s^{-1}. The reverse bias V_R was −6 V and the closing pulse was +6 V. The thermal activation energy of $E_c-0.60$ eV was obtained from the plot of $\ln(e_n/T^2)$ vs $10^3/T$ shown in the inset.

the same rate window of 11.63 s^{-1} for different values of reverse bias. [(a) $V_R=-13$ V, $V_p=+13$ V; (b) $V_R=-6$ V, $V_p=+6$ V; and (c) $V_R=-1$ V, $V_p=+1$ V]. It is clear from the figure that the DLTS peak at $V_R=-1$ V (small electric field) (c) occurs at 292 K, while the DLTS peak at $V_R=-13$ V (large electric field) (a) occurs at 274 K. This is a characteristic signature of field enhanced electron emission rate and this implies that the electron emission rates from the $Z_{1/2}$ center are enhanced by the electric field in the space-charge region.[19]

Figure 3 shows DDLTS spectra (difference spectra); the reverse bias was fixed at −13 V. The two filling pulses V_{p1}

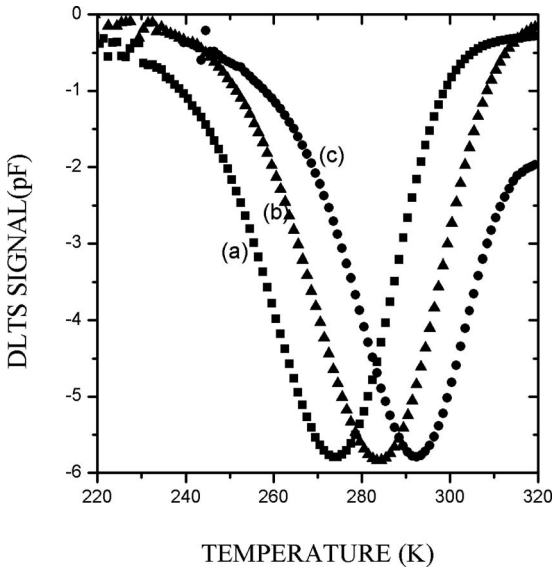

FIG. 2. DLTS spectra of the $Z_{1/2}$ level in electron irradiated 4*H*-SiC samples for the same rate window of 11.63 s^{-1} at three different reverse bias voltages (i.e., three different electric fields): (a) $V_R=-13$ V, $V_p=+13$ V; (b) $V_R=-6$ V, $V_p=+6$ V; (c) $V_R=-1$ V, $V_p=+1$ V.

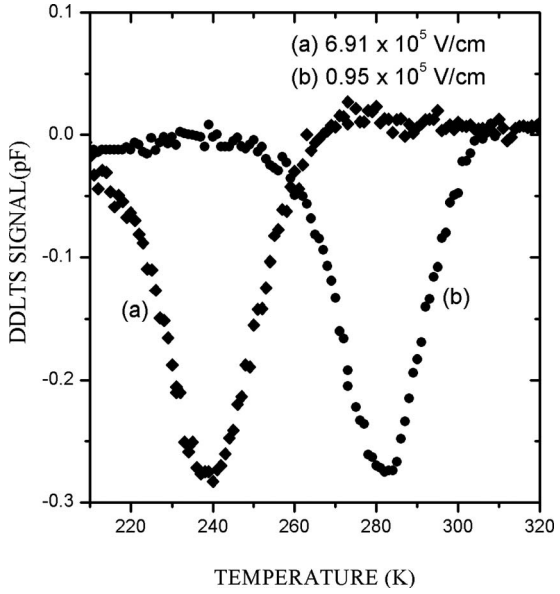

FIG. 3. DDLTS spectra of the $Z_{1/2}$ level in electron irradiated 4*H*-SiC for a rate window of 4.65 s^{-1} at a fixed reverse bias of −13 V. (a) $V_{p1}=12.0$ V and $V_{p2}=12.6$ V. (b) $V_{p1}=2.0$ V and $V_{p2}=2.6$ V.

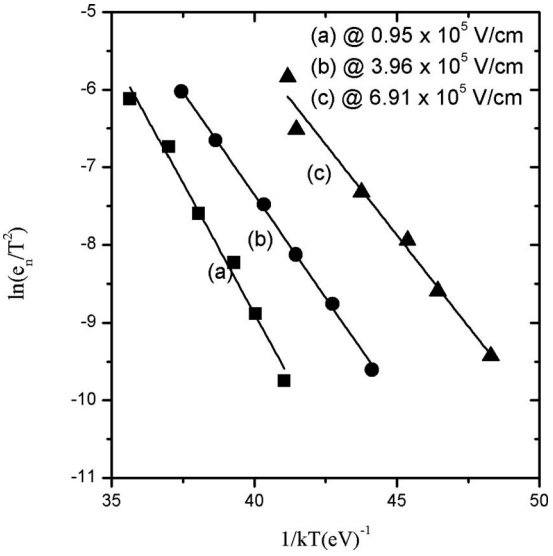

FIG. 5. The plot of $\ln(e_n/T^2)$ vs $1/kT$ at constant fields; the activation energy was obtained from the slope of these lines. (a) $F=0.95\times10^5$ V/cm with $E_c-0.67$ eV. (b) $F=3.96\times10^5$ V/cm with $E_c-0.53$ eV. (c) $F=6.91\times10^5$ V/cm with $E_c-0.47$ eV.

and V_{p2} are 12.0 and 12.60 V, respectively, for curve (a) and 2.0 and 2.6 V for curve (b). For the same rate window of 4.65 s^{-1}, the peaks occur at 40 K apart. By varying V_{p1} and V_{p2} but keeping $\Delta V_p=0.6$ V and V_R fixed, measurements of emission rates are made at different fields within the depletion region.

In Fig. 4, we show the dependence of emission rate from the $Z_{1/2}$ center on the electric field for a given temperature. The plot shows this dependence at three selected temperatures of 270, 285, and 300 K. At 300 K, as an example, the emission rate increased from 33.53 s^{-1} at $F=1.39\times10^5$ V/cm to 260.60 s^{-1} at $F=5.35\times10^5$ V/cm. The emission rate is indeed enhanced by the electric field in the junction. The activation energy of $Z_{1/2}$ centers can be determined as a function of electric field at the junction. The difference spectrum is recorded at different rate windows similar to the standard DLTS technique and the Arrhenius plot of ln (e_n/T^2) versus $1/kT$ is made to determine the activation energy of the defect at this particular electric field. Figure 5 shows the plot of ln (e_n/T^2) versus $1/kT$ at selected electric fields. We obtain, from the plot, an activation energy of $E_c-0.67$ eV at an electric field of 0.95×10^5 V/cm, an activation energy of $E_c-0.53$ eV at an electric field of 3.96×10^5 V/cm, and an energy of $E_c-0.47$ eV at $F=6.91\times10^5$ V/cm. Clearly the activation energy of the $Z_{1/2}$ centers depends on the electric field at which it was determined. Figure 6 illustrates the variation in the activation energy with the electric field. It shows a linear relationship

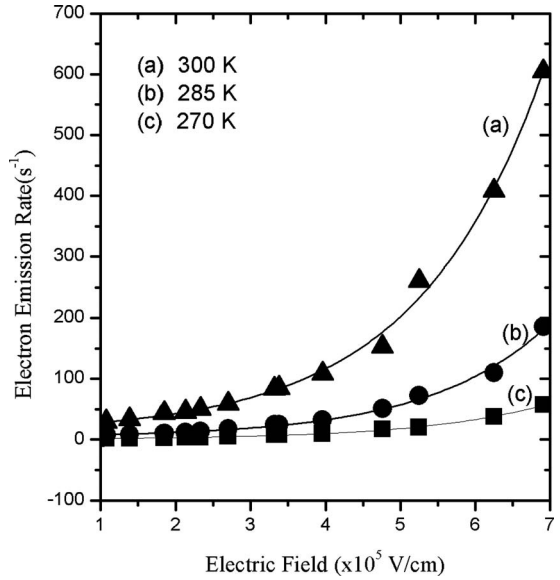

FIG. 4. The dependence of electron emission rates from $Z_{1/2}$ at three selected temperatures vs the electric field in the depletion region of a reverse-biased ($V_R=-13$ V) electron irradiated 4*H*-SiC sample.

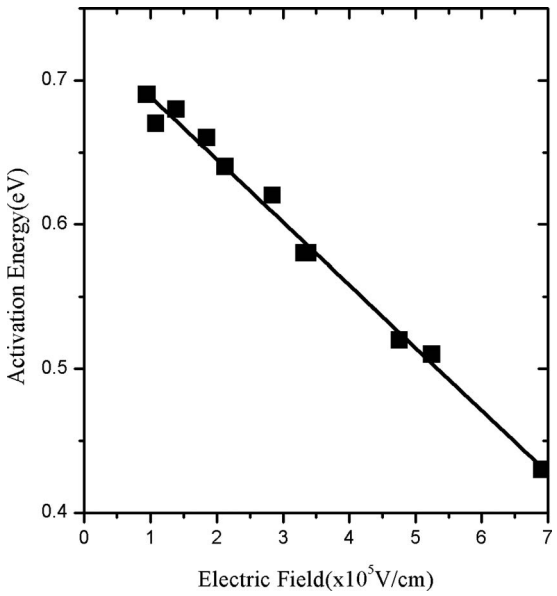

FIG. 6. Variation in the activation energy with the electric field at which it is determined. The activation energy is $E_c-0.72$ eV at zero field ($F=0$).

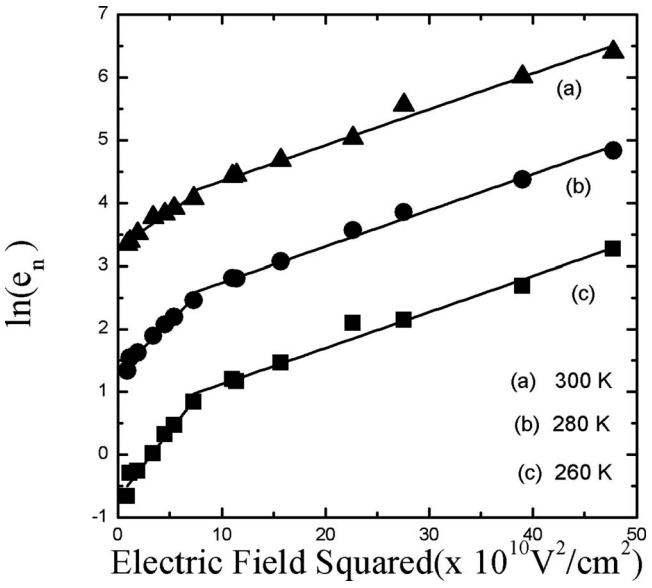

FIG. 7. A plot of $\ln(e_n)$ vs the square of the electric field. The data points are grouped into two stages. The data in each stage can be fitted with a straight line with different slopes. A two stage tunneling process is suggested.

between the activation energy and the field at which it was measured. The extrapolation of the straight through the data points to zero, as shown in Fig. 6, gives the activation energy at zero field ($F=0$). In this case, the estimated activation energy at zero field is 0.72 eV. The dependence of activation energies of *DX* level in GaAlAs and of the Ti level in InP:Ti on electric field has been reported.[20,21] The results presented in Figs. 2–6 clearly demonstrate the electric field enhancement of emission rates from $Z_{1/2}$ centers. This enhancement can be understood in terms of phonon assisted tunneling mechanism. In the Karpus and Perel[22–24] phonon assisted tunneling model, the emission rate is given by

$$e_n(F) = e_{no} \exp\left(\frac{F^2}{F_c^2}\right), \tag{1}$$

where the critical field F_c is given by

$$F_c = \sqrt{\frac{3m^*\hbar}{q^2\tau_2^3}},$$

where τ_2 is the temperature dependent tunneling time and m^* is the effective mass of the charge carrier.

$$\tau_2 = \frac{\hbar}{2k_BT} \pm \tau_1, \tag{2}$$

where the plus and minus signs correspond to the adiabatic potential structures of substitutional impurities and autolocalized centers, respectively, and τ_1 is the time constant which is of the order of the inverse local impurity vibration frequency.[25,26]

According to Eq. (1), a plot of the logarithm of the emission rates as a function of the square of the electric field ought to produce a straight line. Figure 7 shows the plot of the logarithm of the emission rate as a function of the square of the electric field at three selected temperatures (260, 280, and 300 K). The experimental data points can be fitted with

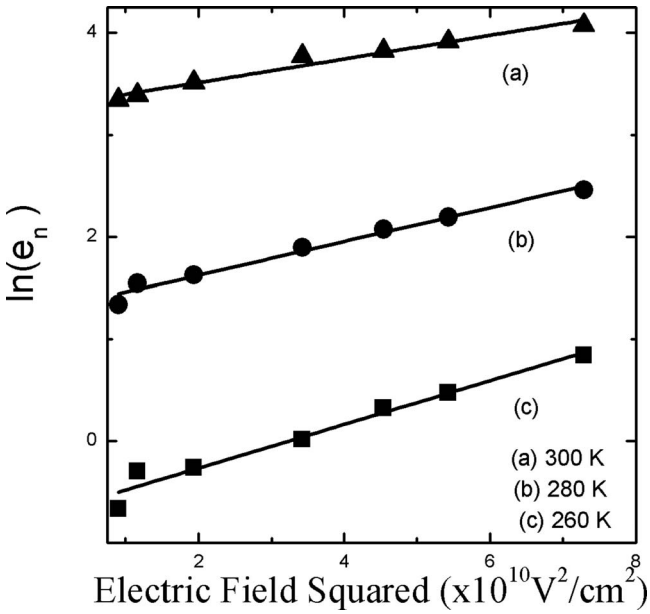

FIG. 8. The variation in $\ln(e_n)$ in stage 1 vs the square of the electric field (from 0.90×10^{10} to 8.06×10^{10} V^2/cm^2) at selected temperatures: (a) 300 K, (b) 280 K, and (c) 260 K. The straight lines through the data points suggest that the phonon assisted tunneling mechanism provides explanation for the enhancement of the emission rates.

a straight line from 0.9×10^{10} to 8×10^{10} V^2/cm^2 (stage 1) and another straight line from 8×10^{10} to 48×10^{10} V^2/cm^2 (stage 2). The straight lines have different slopes. It appears that there are two processes taking place simultaneously: one dominating in stage 1 ($0.9\times10^{10}\leq F^2\leq8\times10^{10}$ V^2/cm^2) and the other more significant in stage 2 ($8\times10^{10}\leq F^2\leq48\times10^{10}$ V^2/cm^2). The data are now replotted in Figs. 8 and 9 to display the two stage process. Figure 8 is the plot of $\ln(e_n)$ versus F^2 at 260, 280, and 300 K. The range of F^2 in this plot is from 0.9×10^{10} to 8×10^{10} V^2/cm^2 and in Fig. 9, the square of the electric field

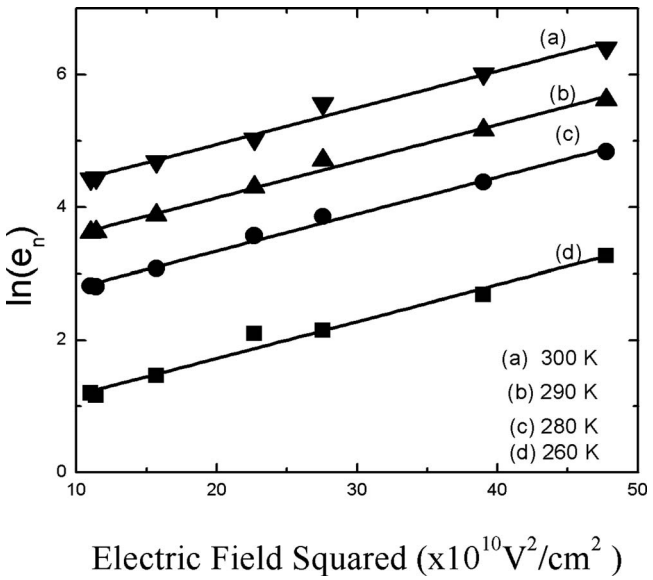

FIG. 9. The variation in $\ln(e_n)$ in stage 2 vs the square of the electric field (from 10×10^{10} to 50×10^{10} V^2/cm^2) at (a) 300 K, (b) 290 K, (c) 280 K, and (d) 260 K.

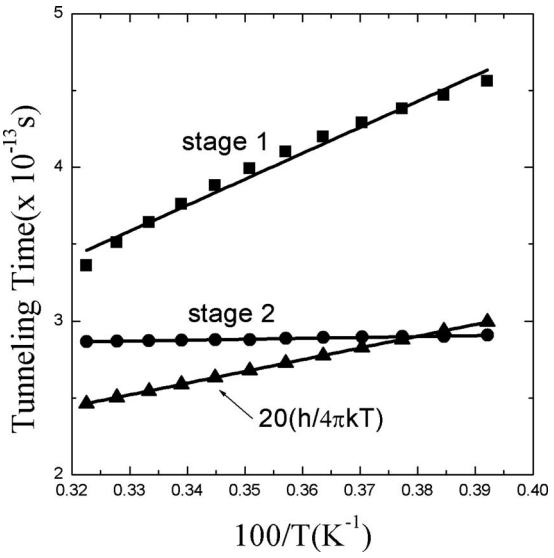

FIG. 10. A plot of tunneling time τ_2 as a function of inverse temperature. The values of τ_2 for both stages were calculated from Figs. 8 and 9. The tunneling time for both stages follows $1/T$ dependence.

varies from 8×10^{10} to 33×10^{10} V^2/cm^2. It is clear that good straight line fits are produced through the data points in both Figs. 8 and 9. This fact confirms that the observed enhancement of the emission rates is adequately described by the phonon assisted model of Karpus and Perel. The values of the critical field, F_c, is determined from the slopes of the straight lines in Figs. 8 and 9, which are equal to $(q^2\tau_2^3)/(3m^*\hbar)$. The tunneling time is then calculated as a function of temperature. The data yield two tunneling times, each corresponding to each stage. It has been stated earlier that the $Z_{1/2}$ center consists of a pair of defects (Z_1 and Z_2) whose electrical levels (the acceptor levels) cannot be resolved. But phonon assisted tunneling times from closely spaced electrical levels may be different. Any small difference in tunneling times can be resolved because the emission rate depends exponentially on the cube of the tunneling time, i.e., $e_n=e_{no}\exp(F^2q^2\tau_2^3/3m^*\hbar)$.

The two stages in Fig. 7 may be due to the difference in tunneling times from Z_1 and Z_2 defects.

We show in Fig. 10 the temperature dependence of the tunneling time τ_2 for both stages. Stage 2 varies weakly with temperature; it varies from 2.91×10^{-13} s at 255 K to 2.87×10^{-13} s at 300 K. For the purpose of comparison, the plot of $\hbar/2k_BT$ (multiplied by 20) is shown in Fig. 10. The tunneling time τ_2 in both stages follows the $1/T$ temperature dependence according to Eq. (2). It is unambiguously clear that τ_2 (for both stages) versus $1/T$ line lies above the $\hbar/2k_BT$ versus $1/T$ line. It has been suggested[26,27] that the tunneling time versus $1/T$ line of carriers from substitutional defects lies above the $\hbar/2k_BT$ line while the tunneling time versus $1/T$ line of carriers from autolocalized defects lie below the $\hbar/2k_BT$ line. This suggests that substitutional defects can be distinguished from autolocalized impurities by measuring the phonon assisted tunneling times. Based on this criterion and from Fig. 10, we suggest that $Z_{1/2}$ is a substitutional defect.

IV. CONCLUSION

Using DLTS and DDLTS, we measured the electron emission rates from the $Z_{1/2}$ defect centers induced by electron irradiation of heavily doped ($\sim10^{17}$ cm^{-3}) 4*H*-SiC bulk samples. The data provide an unambiguous evidence of electric field enhancement of emission rates from $Z_{1/2}$ centers. As a consequence of the influence of the electric field in the depletion region, the activation energy of the defect level varies from $E_c-0.72$ eV at zero field to $E_c-0.47$ eV at 6.9×10^5 V/cm. This suggests that great care must be exercised when interpreting all data obtained by DLTS measurements when the doping level exceeds 10^{15} cm^{-3}. The phonon assisted tunneling model provides adequate explanation for the experimental data. The model is identified by plotting the logarithm of the emission rates versus the square of the electric field in the junction. Further analysis of the data reveals two tunneling stages with two different tunneling times τ_2. This may be as a result of small differences in tunneling times from Z_1 and Z_2 defects which can be resolved. The tunneling time τ_2 for each stage follows the $1/T$ relationship. At any given temperature T, the values of the tunneling times are larger than $\hbar/2k_BT$. As a consequence, we suggest that the $Z_{1/2}$ defect is a substitutional defect in 4*H*-SiC.

ACKNOWLEDGMENTS

The authors would like to acknowledge the technical assistance of Gerald Landis and the assistance of Dr. Rex Berney in constructing the platform for the cryostat.

[1]T. Dalibor, C. Peppermuller, G. Pensl, S. Sridhara, R. P. Devaty, W. J. Choyke, A. Itoh, T. Kimoto, and H. Matsunami, Inst. Phys. Conf. Ser. **142**, 517 (1996).
[2]T. Kimoto, A. Itoh, T. Dalibor, C. Peppermuller, and G. Pensl, Appl. Phys. Lett. **67**, 2833 (1995).
[3]T. Dalibor, G. Pensl, H. Matsunami, T. Kimoto, W. J. Choyke, A. Schoner, and N. Nordell, Phys. Status Solidi A **162**, 199 (1997).
[4]C. Hemmingsson, N. T. Son, O. Kordina, J. P. Bergman, E. Janzen, J. L. Lindstom, S. Savage, and N. Nordell, J. Appl. Phys. **81**, 6155 (1997).
[5]D. Åberg, A. Hallén, and B. G. Svensson, Physica B **273–274**, 672 (1999).
[6]J. P. Doyle, M. K. Linnarsson, P. Pellegrino, N. Keskilalo, B. G. Svensson, A. Schoner, N. Nordell, and J. L. Lindstrom, J. Appl. Phys. **84**, 1354 (1998).
[7]C. Hemmingsson, N. T. Son, A. Ellison, J. Zhang, and E. Janzen, Phys. Rev. B **58**, R10119 (1998); **59**, 7768(E) (1999).
[8]A. Kawasuso, F. Redman, R. Krause-Rehbergy, M. Weidner, T. Frank, G. Pensl, P. Sperr, W. Triftshauser, and H. Itoh, Appl. Phys. Lett. **79**, 3950 (2001).
[9]K. Fujihira, T. Kimoto, and H. Matsunami, Appl. Phys. Lett. **80**, 1586 (2002).
[10]I. Pintilie, L. Pintilie, K. Irmscher, and B. Thomas, Appl. Phys. Lett. **81**, 4841 (2002).
[11]C. G. Hemmingsson, N. T. Son, and E. Janzen, Appl. Phys. Lett. **74**, 839 (1999).
[12]L. Storasta, J. P. Bergman, E. Janzen, A. Henry, and J. Lu, J. Appl. Phys. **96**, 4909 (2004).
[13]G. Alfieri, E. V. Monakhov, B. G. Svensson, and M. K. Linnarsson, J. Appl. Phys. **98**, 043518 (2005).
[14]T. A. G. Eberlein, R. Jones, and P. R. Jones, Phys. Rev. Lett. **90**, 225502 (2003).
[15]J. Frenkel, Phys. Rev. **54**, 647 (1938).
[16]A. Castaldini, A. Cavallini, and L. Rigutti, Semicond. Sci. Technol. **21**, 724 (2006).
[17]H. Lefevre, and M. Schule, Appl. Phys. **12**, 45 (1977).

[18]P. Blood, Semicond. Sci. Technol. **1**, 7 (1986).
[19]U. S. Qurashi, M. Z. Igbal, C. Delerue, and M. Lannoo, Phys. Rev. B **45**, 13331 (1992).
[20]M. Zazoui, S. L. Feng, and J. C. Bourgoin, Semicond. Sci. Technol. **6**, 973 (1991).
[21]N. Baber, H. Scheffler, A. Ostmann, T. Wolf, and D. Bimberg, Phys. Rev. B **45**, 4043 (1992).
[22]V. Karpus and V. I. Perel, Sov. Phys. JETP **64**, 1376 (1986).
[23]S. D. Ganichev and W. Pretti, Phys. Solid State **39**, 1703 (1997).
[24]D. Pons and S. Makram-Ebeid, J. Phys. (Paris) **40**, 1161 (1979).
[25]S. D. Ganichev, Physica B **273–274**, 737 (1999).
[26]S. D. Ganichev, E. Ziemann, I. N. Yassievich, A. A. Istratov, and E. R. Weber Phys. Rev. B **61**, 10361 (2000); S. D. Ganichev, W. Prettl, and P. G. Huggard, Phys. Rev. Lett. **71**, 3882 (1993).
[27]V. P. Markevich, A. R. Peaker, V. V. Litvinov, L. I. Murin, and N. V. Abrosimov, Physica B **376–377**, 200 (2006).